Tellus (1997), 49A, 337–346
Printed in UK – all rights reserved

TELLUS
ISSN 0280–6495

A note on 1-dimensional calculations of baroclinic and barotropic instabilities

By PETER D. DITLEVSEN, *Niels Bohr Institute, Geophysical Department, Juliane Maries Vej 30, 2100 Copenhagen Ø, Denmark*

(Manuscript received 17 July 1996; in final form 25 October 1996)

ABSTRACT

Linear instability of zonal jets are calculated within the framework of the quasi-nondivergent potential vorticity equation. The vertical structure of the flow is treated using vertical normal mode expansion. Three simple 1-dimensional cases are investigated. Firstly, the baroclinic flow on the β-plane, where instability is seen as function of the shape and strength of a jet mimicking the vertical structure of a typical zonal jet in the atmosphere. The study shows that the jet is most unstable for a low-lying jetmaximum. Secondly, a purely barotropic flow on a β-plane, with fixed boundaries in north and south and with periodic boundaries in east-west, mimicking the west wind belt is investigated. In this simple case, the linearized instability equation is solved both spectrally and using finite differences in order to illustrate the dependence on resolution. The stability of the jet is independent on the position within the channel. Finally, for each vertical normal mode, equivalent to a barotropic flow, the stability of a typical west-wind jet on the sphere is calculated. In this case, the jet is more stable the further away from the equator, thus the Coriolis force stabilizes the flow. These very simple examples are in general agreement with findings from full 3-dimensional stability analysis.

1. Introduction

The quasi-geostrophic approximation has, although far from having predictive power, proven itself capable of reproducing and explaining quite well the general dynamics and energetics of the atmosphere.

The main mechanisms for maintaining the general circulation in the atmosphere can to a large extent be understood in terms of classical linear instability analysis.

In the atmosphere, the dominant flow-pattern in the midlatitudes, is energetically maintained by the pole-ward transportation of heat and momentum. This transport is maintained by the Rossby waves of the west-wind belt.

There are basically 2 possible instability mechanisms responsible for this transport, the baroclinic instability, depending on the thermal, or vertical, wind-shear, and the barotropic instability depending on the horizontal wind-shear.

The classical "constant thermal shear" models by Eady (1949) and Charney (1947) show, by a linear stability analysis, that the unstable atmospheric waves in the east-west direction are of wavenumbers 5–10, corresponding to a wavelength of 2000–4000 km. Green (1960) and Burger (1962) showed that there are in fact unstable modes everywhere in the considered phase space, but still dominated by the Charney instabilities.

The barotropic instability of a horizontal "cosine jet" on a β-plane was investigated by Kuo (1979). It was found that with realistic values of the zonal jet the growth rate of the unstable modes are slower than that for the baroclinic models. It was also found that the β-effect tends to stabilize the flow.

Kasahara and Tanaka (1989) have studied the baroclinic instability of a flow with a linear vertical wind profile using the vertical normal expansion. Their findings are in good agreement with the much simpler Charney model.

The dominating waves seen in the west-wind belts are wavenumbers 3–6. This is also seen in the numerical circulation models. So in this scenario it is conjectured that the interaction between the unstable modes, wavenumbers 6–10, and the longer waves, wavenumbers 3–6, will dominate when the linear expansion is no longer valid, and the energy will flow from the short waves to the long waves. The long waves will, when they have build up, be more efficient in the pole-ward heat transfer than the short waves.

A vast literature on instabilities in the atmosphere exists, for a review see Grotjahn (1984). Some classical references for modern 3-dimensional instability analysis are Frederiksen (1978), Simmons and Hoskins (1976) and Grotjahn (1987). A good textbook also treating Reynold and other criteria for instability is Pedlosky (1987).

The work presented in this note is by no means pretended to contribute to the detailed and accurate 3-dimensional instability analysis performed by others. It should also be noted that more modern approaches to growth of perturbations and predictability, like singular vector analysis (Palmer et al., 1994) and breeding vectors (Toth and Kalney, 1993) is beyond any simple instability analysis. The motivation for this study is merely to see within the framework of the simple 1-dimensional calculations the roles of baroclinic versus barotropic instabilities of typical zonal flows. The simplicity of the 1-dimensional case makes it easy to understand exactly which instability mechanism is at play. We will consider the stability of zonal jets as a function of the shape of the jet. Firstly, we consider baroclinic instability of a jet as determined by the height and width of the jet, and secondly, the equivalent barotropic instability of a midlatitude zonal flow on the sphere also as a function of the shape of basic flow. In both cases we assume the static stability to be simply inversely proportional to the square of the pressure, which has been shown to be a fair approximation to the real atmosphere (Wiin-Nielsen and Marshall, 1990).

In order to illustrate the sensitivity of the numerical solution to the resolution, we solve the barotropic case of a simple channel stream both spectrally and by finite differences. we find that the convergence, as a function of resolution, is rather slow in the finite differences case. Furthermore, we find, in both cases differences in convergence depending on whether we truncate at an odd or an even number, called an odd/even oscillation.

2. Linear instability analysis

In the quasi-geostrophic approximation, the basic equations are, by eliminating ω between the vorticity equation and the thermodynamic equation, combined to the usual equation of conserved quasi-nondivergent potential vorticity (Kasahara and Tanaka, 1989):

$$\frac{\mathrm{d}Q}{\mathrm{d}t} = \frac{\mathrm{d}}{\mathrm{d}t}\left(\zeta + f + \frac{\partial}{\partial p}\left(\frac{f_0^2}{\sigma}\frac{\partial \psi}{\partial p}\right)\right) = 0, \tag{1}$$

where $\mathrm{d}/\mathrm{d}t = \partial/\partial t + \boldsymbol{v}\nabla$, $\boldsymbol{v}$ is the horizontal nondivergent wind. Data studies of the atmosphere show that the static stability can be approximated with

$$\sigma \equiv -\alpha\frac{\partial \ln \Theta}{\partial p} = \frac{\sigma_0}{p_*^2}, \tag{2}$$

where $\alpha = 1/\rho$ and $p_* = p/p_0$. We will in the following omit the subscript $_*$, so that $0 < p < 1$ is the normalized pressure.

In order to investigate the stability of a given stationary flow, $\psi_0(\boldsymbol{x}, p)$, fulfilling (1), $\boldsymbol{x}$ being the horizontal coordinate, we apply a perturbation of the form, $\psi_1 = \psi_1(\boldsymbol{x}, p)\exp(-ict)$, and linearize (1) around ψ_0 by neglecting second-order terms in the perturbation ψ_1. From this linear equation we seek solutions that grow exponentially in time, that is solutions with $\mathrm{Im}(c) > 0$. If such solutions, ψ_1, exist, the basic flow, ψ_0, will be unstable, feeding energy into ψ_1 as long as the linear approximation holds ($|\psi_1| \ll |\psi_0|$).

The linear differential equation is solved spectrally, by expanding the stream functions in a normal mode basis,

$$\psi(\boldsymbol{x}, p) = \sum_i \psi_i(\boldsymbol{x})\varepsilon_i(p). \tag{3}$$

The vertical structure functions, $\varepsilon_i(p)$, we will use are the normal modes obtained by imposing the simplest possible boundary conditions, namely ω vanishing at the top and bottom of the atmosphere, to the following vertical mode structure equation,

$$\frac{\mathrm{d}}{\mathrm{d}p}\left(\frac{f_0^2}{\sigma}\frac{\mathrm{d}\varepsilon}{\mathrm{d}p}\right) + \lambda^2\varepsilon = q^2\frac{\mathrm{d}}{\mathrm{d}p}\left(p^2\frac{\mathrm{d}\varepsilon}{\mathrm{d}p}\right) + \lambda^2\varepsilon = 0, \tag{4}$$

$$\frac{\mathrm{d}\varepsilon}{\mathrm{d}p} = 0, \qquad p = 1, p_\mathrm{T}.$$

$p_T > 0$ is the pressure at the top of the atmosphere (arbitrarily close to zero), and $q^2 \equiv f_0^2/\sigma_0 p_0^2$. The normal mode solutions to (4) are,

$$\varepsilon_0(\xi) = 1/\sqrt{1-\exp(-\xi_T)}, \qquad \lambda_0^2 = 0,$$

$$\varepsilon_n(\xi) = \sqrt{\frac{1}{2\lambda_n^2 \xi_T}}\, e^{\xi/2}\left(\sin\left(n\pi\frac{\xi}{\xi_T}\right) - 2\frac{n\pi}{\xi_T}\cos\left(n\pi\frac{\xi}{\xi_T}\right)\right), \tag{5}$$

$$\lambda_n^2 = \left(\frac{n\pi}{\xi_T}\right)^2 + \frac{1}{4},$$

with $\xi \equiv \log(p)$. ε_0 is called the external mode, and $\varepsilon_n(p)$, $n > 0$ are the internal modes. From (5) it is seen that we need to specify the (arbitrary) top level pressure $p_T > 0$, at which $\omega = 0$. This corresponds to having a "lid" on the atmosphere. The choice of vertical normal mode basis is in principle arbitrary, it only influences the result of the analysis through the convergence as function of the number of modes included. Kasahara and Tanaka uses a slightly different basis, governed by the lower boundary condition $d\varepsilon/dz = 0$ at $z = 0$. The first few vertical eigenmodes are shown in Fig. 1.

3. Baroclinic instability

Firstly we will study the stability of a jet in the vertical wind profile. For this purpose we take the horizontal geometry to be a plane, where we apply the β-plane approximation at the midlatitude, $f \approx f_0 + \beta(y - y_0)$. This treatment follows closely the model used by Kasahara and Tanaka, where a linear vertical wind profile was investigated.

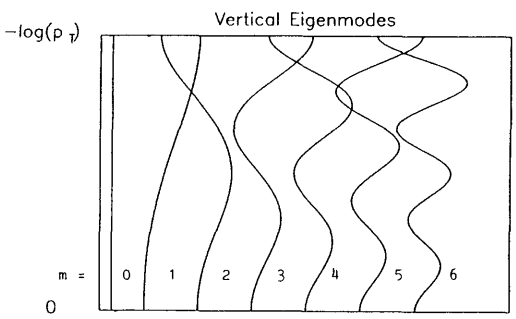

Fig. 1. The external and the first six internal vertical eigenmodes.

The stream function is specified as,

$$\psi = -U(p)y + \hat{\psi}(p)\, e^{ik(x-ct)}, \tag{6}$$

where $-U(p)y$ is the basic state stream function, $U(p) = -\partial\psi/\partial y$, trivially fulfilling (1), and the last term is the perturbation. This form is then inserted into (1), and we get,

$$\frac{\partial}{\partial t}\left(\nabla^2\psi + f + q^2\frac{\partial}{\partial p}\left(p^2\frac{\partial\psi}{\partial p}\right)\right) + v\cdot\nabla\left(\nabla^2\psi + f + q^2\frac{\partial}{\partial p}\left(p^2\frac{\partial\psi}{\partial p}\right)\right)$$
$$= \left(ick^3\hat{\psi} - ick^3\frac{q^2}{k^2}\frac{d}{dp}\left(p^2\frac{d\hat{\psi}}{dp}\right) - ik^3U\hat{\psi} + ik^3U\frac{q^2}{k^2}\frac{d}{dp}\left(p^2\frac{d\hat{\psi}}{dp}\right)\right)$$
$$+ ik^3\frac{\beta}{k^2}\hat{\psi} - ik^3\frac{q^2}{k^2}\hat{\psi}\frac{d}{dp}\left(p^2\frac{dU}{dp}\right)\Bigg) e^{ik(x-ct)} = 0, \tag{7}$$

where second order terms in $\hat{\psi}$ are neglected. The stream functions are expanded in vertical normal modes,

$$\hat{\psi}(p) = \sum_i \psi_i\varepsilon_i(p), \qquad U(p) = \sum_i U_i\varepsilon_i(p). \tag{8}$$

Then (7) becomes, by use of (4),

$$\sum_i\left(c\left(1+\frac{q^2}{k^2}\lambda_i^2\right)\psi_i - \sum_j\left(1+\frac{q^2}{k^2}\lambda_i^2 - \frac{q^2}{k^2}\lambda_j^2\right)\psi_i U_j\varepsilon_j - c_R\psi_i\right)\varepsilon_i = 0, \tag{9}$$

where we have defined the Rossby speed, $c_R \equiv \beta/k^2$. By multiplying (9) by ε_l and integrating vertically, utilizing the orthonormality of the vertical modes, we finally arrive at the eigenvalue equation,

$$\sum_i\left(\sum_j \frac{1+(q/k)^2(\lambda_i^2-\lambda_j^2)}{1+(q/k)^2\lambda_l^2}U_j I(i,j,l) - \frac{c_R}{1+(q/k)^2\lambda_l^2}\delta_{il}\right)\psi_i = c\psi_l. \tag{10}$$

δ_{kl} is the Kronecker symbol, and the interaction

integral is defined as,

$$I(i,j,k) = \int_1^{p_T} \varepsilon_i \varepsilon_j \varepsilon_k \, dp$$
$$= \int_0^{\xi_T} e^{-\xi} \varepsilon_i(\xi) \varepsilon_j(\xi) \varepsilon_k(\xi) \, d\xi. \quad (11)$$

3.1. The basic state profile

The U profile is taken to be of the form,

$$U(p) = U_0 \frac{p^{\alpha_1}(1-p)^{\alpha_2}}{p_0^{\alpha_1}(1-p_0)^{\alpha_2}}, \quad (12)$$

where $p_0 = \alpha_1/(\alpha_1 + \alpha_2)$ is the pressure level of the wind maximum. The parameters U_0, α_1 and α_2 are then varied such that the instability of the jet is calculated as a function of the strength, the broadness and the position of the jet independently.

The constants we use in the calculations are,

$$\beta = 1.6 \times 10^{-11} \text{ m}^{-1} \text{ s}^{-1} = 1.38 L^{-1} \text{ day}^{-1}$$

$$q^2 = \frac{f_0^2}{\sigma_0 p_0^2} = 1.25 \times 10^{-12} \text{ m}^{-2} = 1.25 L^{-2}$$

$$a = 6.37 \times 10^6 \text{ m} = 6.37 L$$

$$\Omega = 7.29 \times 10^{-5} \text{ s}^{-1} = 2\pi \text{ day}^{-1}$$

with a natural length scale, $L = 1000$ km.

The eigenmode expansion (8) is truncated at $N = 36$, where the results are fairly converged as a function of the truncation. The growth rate, $k \, \text{Im}(c)$, for the most unstable mode, is shown in Fig. 2. The results shown in the uppermost panel is quite similar to what is found in the case of a linear wind profile (Kasahara and Tanaka, 1989). This indicates that the instability is governed by the linear shear on the bottom side of the jet. The middle panel shows that there is little influence on the stability from having a narrower jet around 200 hPa, on the contrary we find that the broad jet is the most unstable. This is due to the fact that the broad jet indeed has a large shear in the lower part of the atmosphere, which dominates the behavior. The third panel clearly shows that the lower the jet maximum the more unstable it becomes. So we find that the baroclinic instability is largest for a low-lying jet. This is what one would expect from the fact that the static stability increase with height.

Green (1960) found, by re-examining Charney's model, instabilities, although weak, also in the areas that Charney found to be stable. It was shown rigorously by Burger (1962) that the Charney problem did have instabilities everywhere, except for a discrete set of points in the parameter space. In Fig. 2, we have for clarity only shown the Charney type of instabilities. These are anyway the only ones with relevance for development of baroclinic waves in the atmosphere. Fig. 3 shows the separation between the Charney- and the Green types of instability. By examining the most unstable eigenmode we find that it will in general grow on the upper side of the jet.

4. Barotropic instability

4.1. Channel stream

Before turning our attention to the problem of barotropic instability on the sphere, we will consider the much simpler case of a periodic channel geometry with the β-plane approximation. Neglecting any vertical structure we have,

$$\frac{d}{dt}(\zeta + \beta y) = \frac{\partial}{\partial t}(\zeta) + J(\psi, \zeta) + \beta \frac{\partial \psi}{\partial x} = 0, \quad (13)$$

where J is the Jacobian. The stream function is chosen as,

$$\psi = \psi_0 + \psi_1 = -\int^y U_0(\tilde{y}) \, d\tilde{y} + \psi_1(y) \, e^{ik(x-ct)}. \quad (14)$$

With the boundary condition that the stream function, $\psi_1(y)$, vanishes on the northern and southern boundaries, the basis in spectral space is simply taken to be,

$$\varepsilon_{m,n}(\tilde{x}, \tilde{y}) = \sin m\tilde{y} \, e^{in\tilde{x}}, \quad (15)$$

with $\tilde{y} = y\pi/D$ and $\tilde{x} = x\pi/L$, D and L are the width and length of the channel, respectively. With $\tilde{c} = cL/2\pi$, $\tilde{k} = 2kD/L$ and $\tilde{\beta} = \beta D^2/\pi$, we obtain the eigenvalue equation:

$$\sum_{j=1}^{N} \left(\sum_{l=1}^{N} 2 \left(\frac{k^2 + n^2 - l^2}{k^2 + m^2} I(j,l,m) U_l^0 \right) - \left(\frac{\tilde{\beta}}{k^2 + j^2} \right) \delta_{jm} \right) \psi_j = \tilde{c} \psi_m, \quad (16)$$

with U_l^0 being the spectral components of the basic state wind, U_0. The interaction integrals are

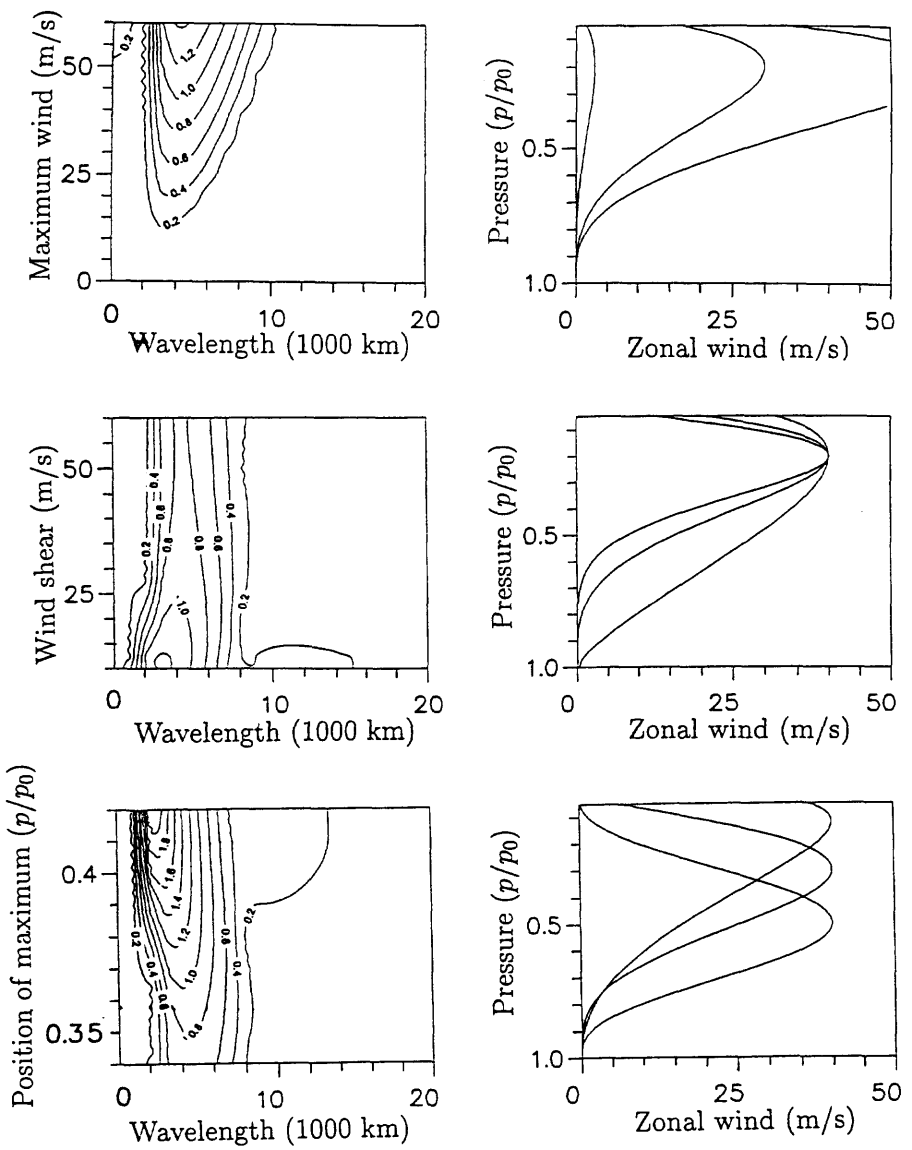

Fig. 2. Baroclinic instability: The growth rate, $k\,\mathrm{Im}(c)$, as function of wavenumber and basic state wind profile, in days^{-1}. Top panel: changing wind maximum at 200 hPa, keeping the curvature at the maximum constant, y-axis coordinate is $U_{\max}$ (m/s). Middle panel: changing shear at wind maximum with a constant wind maximum at 200 hPa, y-axis coordinate is (negative) curvature at wind maximum. Bottom panel: changing position of wind maximum with a constant curvature, y-axis coordinate is pressure level of wind maximum. The right panels show the basic state wind profiles corresponding to the parameter values at the top, the middle and at the bottom of the left side panels.

given by,

$$I(l,j,m)=\frac{1}{\pi}\int_0^{\pi}\sin ly\sin jy\sin my\,\mathrm{d}y$$
$$=\frac{1}{4\pi}\left(\frac{1-\cos(l-j-m)\pi}{l-j-m}+\frac{1-\cos(l-j+m)\pi}{l-j+m}\right.$$
$$\left.-\frac{1-\cos(l+j-m)\pi}{l+j-m}-\frac{1-\cos(l+j+m)\pi}{l+j+m}\right). \tag{17}$$

In order to see the influence of the numerical

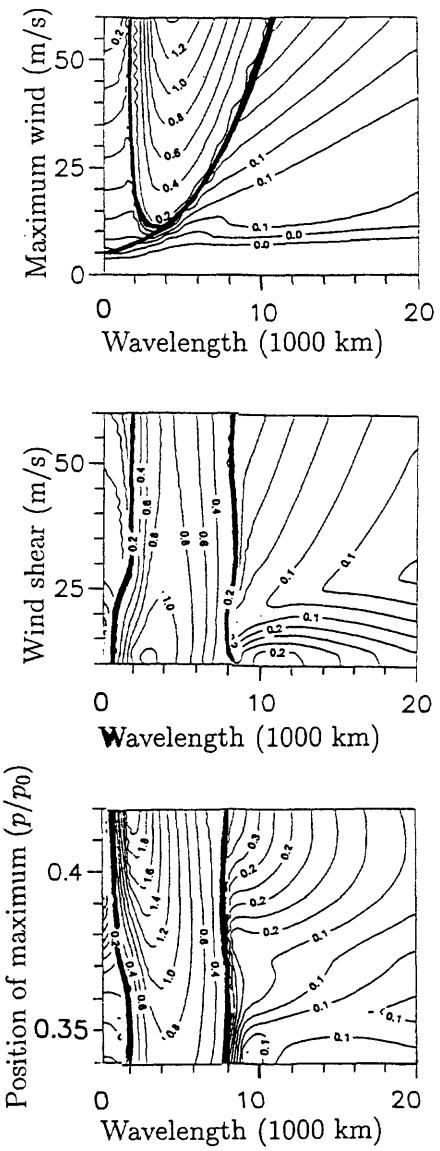

Fig. 3. Growth rate for Charney and Green instability types.

scheme and the truncation, we rewrite the eigenvalue equation using finite differences in the $\tilde{y}$ direction. Defining $\psi_n = \psi(n\Delta)$, with $\Delta = D/N$, we substitute,

$$\frac{\partial}{\partial y}\psi_n \to \frac{1}{2\Delta}(\psi_{n+1} - \psi_{n-1}),$$
$$\frac{\partial^2}{\partial y^2}\psi_n \to \frac{1}{\Delta^2}(\psi_{n+1} + \psi_{n-1} - 2\psi_n). \tag{18}$$

The eigenvalue equation equivalent to (16) then becomes,

$$(\beta\Delta^2 - U^0_{n+1} - U^0_{n-1} + 2U^0_n)A^{-1}_{nm} + U^0_n\delta_{nm})X_m = cX_n, \tag{19}$$

where we have used the transformation,

$$X_n = \psi^0_{n+1} + \psi^0_{n-1} - (2 + k^2\Delta^2)\psi^0_n; \tag{20}$$

A_{mn} is the (symmetric) transformation matrix: $X_m = A_{mn}\psi_n$.

Fig. 4 shows the values of the imaginary part of the eigenvalues of the most unstable mode, corresponding to meridional wavenumber 5. It is seen that they have converged for a truncation around $N = 60$. The ways the two methods converge are quite different, and the results should not be trusted before the convergence is reached. Even when convergence is reached the two results deviate by approximately 5%.

The basic state wind profile, U_0, is taken to be of the form,

$$U_0(y) = U_0 y^{2\alpha_1}(1 - y^2)^{\alpha_2}. \tag{21}$$

The parameters U_0, α_1, α_2 are then chosen such that (1) wind maximum, (2) curvature at wind maximum and (3) position of wind maximum are varied independently. Fig. 5 shows the growth rate of the most unstable mode. We see that wavenumbers 3–7 are the most unstable with respect to increasing zonal wind speed (top panel). In case of narrowing zonal wind profile (middle panel) we find that the wavenumber of the most unstable mode increases slightly with increasing wind shear. Finally, we see that the instability is very little influenced by the position of the zonal wind jet (bottom panel), this means that, in this case, the β effect plays little role in stabilizing the flow.

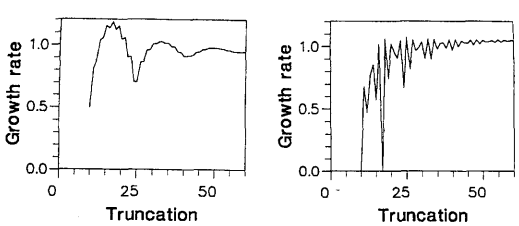

Fig. 4. The imaginary part of the most unstable modes as a function of truncation, N, for a given basic state wind profile. The left panel shows the result in spectral space. The right panel shows the result using finite differences.

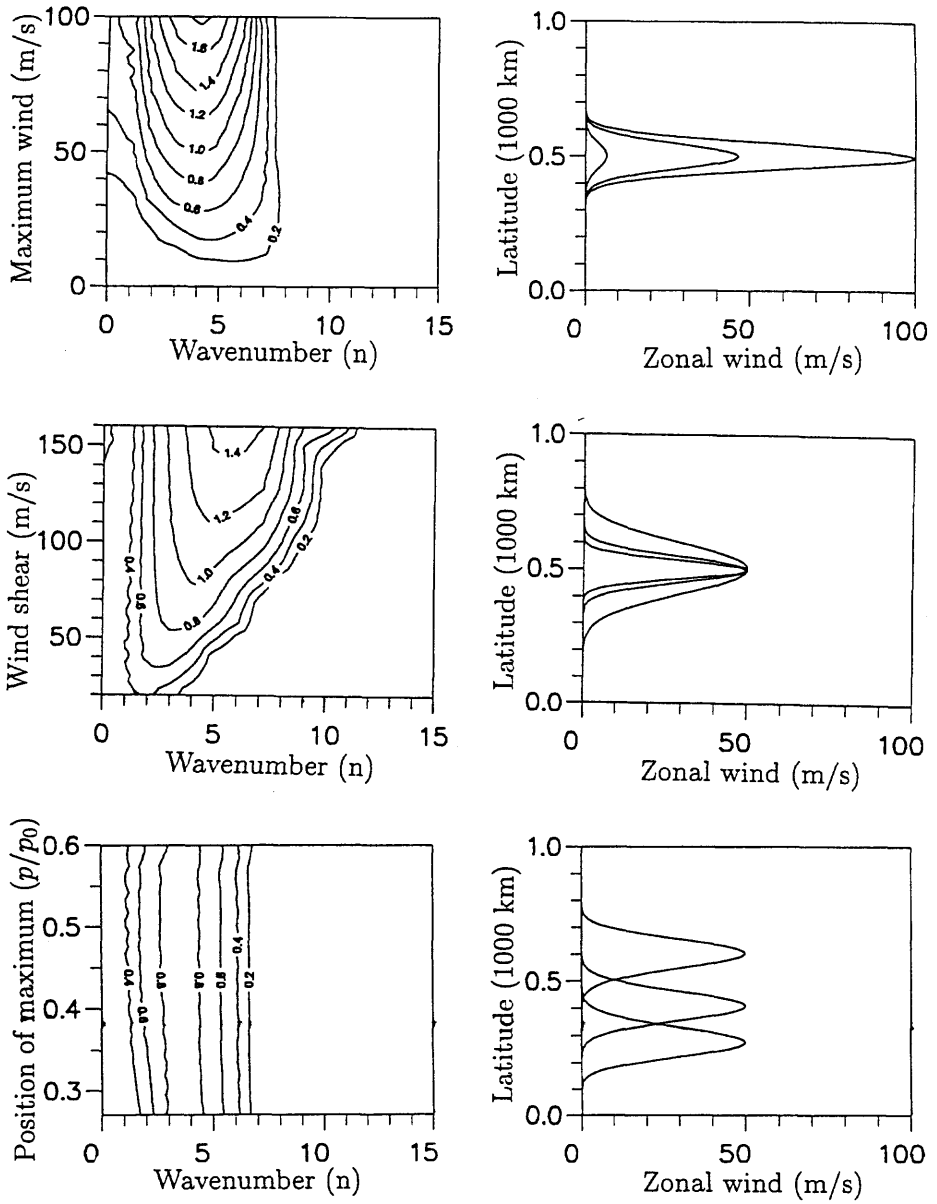

Fig. 5. Barotropic instability in Channel: the growth rate, $k\,\mathrm{Im}(c)$, as function of wavenumber and basic state wind profile (days^{-1}). Top panel: changing wind maximum, keeping the curvature at the maximum constant; y-axis coordinate is U_{max} (m/s). Middle panel: changing shear at wind maximum with a constant wind maximum; y-axis coordinate is curvature at wind maximum. Bottom panel: changing position of wind maximum with a constant curvature.

4.2. Equivalent barotropic instability on the sphere

In this section, we consider the stability of a typical westerly jet on the sphere. Firstly the equation (1) is expressed in spherical coordinates, noting that in the non-divergent case we have for $\psi(\boldsymbol{x}, p) = \psi(\boldsymbol{x})\epsilon_r(p)$,

$$\boldsymbol{v}\cdot\nabla\frac{\partial}{\partial p}\left(p^2\frac{\partial\psi}{\partial p}\right) = k\times\nabla\psi\cdot\frac{\partial}{\partial p}\left(p^2\frac{\partial\nabla\psi}{\partial p}\right) = 0, \quad (22)$$

with $\partial y/\partial\tilde{\psi} = a$, $\tilde{\psi}$ the latitude, $\partial y/\partial\lambda = 0$, $\partial x/\partial\tilde{\psi} = 0$, $\partial x/\partial\lambda = a\cos\tilde{\psi}$, and $\mu \equiv \sin\tilde{\psi}$, (1) becomes,

$$\frac{\partial\zeta}{\partial t} + q^2a^2\frac{\partial}{\partial t}\left(\frac{\partial}{\partial p}\left(p^2\frac{\partial\psi}{\partial p}\right)\right) + \frac{1}{a^2}\left(\frac{\partial\psi}{\partial\lambda}\frac{\partial\zeta}{\partial\mu} - \frac{\partial\zeta}{\partial\lambda}\frac{\partial\psi}{\partial\mu}\right) + \frac{2\Omega}{a^2}\frac{\partial\psi}{\partial\lambda} = 0. \tag{23}$$

The last term is the Coriolis term, using $f = 2\Omega\sin\psi$.

Let the basic stream function be independent of pressure and longitude, thus trivially a stationary solution to (1). Expanded in the Legendre polynomials we have,

$$\psi(\mu) = \sum_n \psi_n P_n(\mu). \tag{24}$$

The perturbation field is defined as,

$$\hat{\psi}(\lambda, \mu, p, t) = \sum_n \hat{\psi}_n \varepsilon_r(p) P_n^m(\mu)\, e^{im(\lambda - ct)}, \tag{25}$$

where m is a specific zonal wavenumber and $\varepsilon_r(p)$ is a vertical eigenmode. Inserting into (23), neglecting second order terms in ψ_n, using the orthogonality of the spherical harmonics, and integrating out the pressure dependency, we obtain the eigenmode equation:

$$\sum_l \left(\left(\sum_n \frac{n(n+1) - l(l+1)}{k(k+1) + q^2\lambda_r^2} J^m(k, l, n)\psi_n\right) - \frac{2}{k(k+1) + q^2\lambda_r^2}\delta_{kl}\right)\hat{\psi}_l = c\hat{\psi}_k, \tag{26}$$

where we have scaled; $\psi \to a^2\Omega\psi$, $q \to aq$, and $c \to \Omega c$. The interaction integral is defined as,

$$J^m(k, l, n) = \int_{-1}^{1} P_k^m(\mu) P_l^m(\mu) \frac{dP_n(\mu)}{d\mu}\, d\mu. \tag{27}$$

With this form of the stream function, we can see from (26) that the pressure dependency becomes trivial. We can rescale the static stability factor as $\sigma_r = \sigma_0\lambda_r^{-2}$, such that higher vertical normal modes correspond to less stable stratification.

4.3. The basic state profile

For the basic state wind we use the simple form,

$$U(\mu) = U_0 \frac{\mu^{2\alpha_1}(1-\mu^2)^{\alpha_2 + 1/2}}{\mu_0^{2\alpha_1}(1-\mu_0^2)^{\alpha_2 + 1/2}}, \tag{28}$$

where $\mu_0 = \alpha_1/(\alpha_1 + \alpha_2 + \frac{1}{2})$ is the location of the wind maximum and $U_0 = U(\mu_0)$ is the maximum wind. The parameters U_0, α_1, α_2 are chosen such that (1) the strength, (2) the width and (3) the position of the jet are varied independently. The truncation is $N = 60$. Fig. 6 shows the growth rate where the vertical component of the perturbation is the external mode, that is, there is no pressure dependency. The situation is rather similar to the case of a channel stream, except for the case shown in the bottom panel. Here we observe that the zonal jet becomes more unstable with respect to position towards the equator, so in this case we see that the Coriolis force stabilize the flow. This is in agreement with the findings of Kuo (1973) in case of a Cosine jet on the β-plane.

Calculationes for the internal vertical modes, $r = 1, 2, \ldots$, shows that the higher vertical wavenumber of the perturbation, the more stable the fluid becomes, and it changes little on which zonal modes are the most unstable. In general the most barotropically unstable modes have zonal wavenumbers 5–10. The form of the most unstable eigenmode shows that the perturbation grows near the jet maximum and on the pole-ward side of the jet. The perturbation will lower the shear of the jet, thus make the flow more stable.

5. Summary

The instability of zonal jet has been investigated in 3 cases. The baroclinic flow on a β-plane, the barotropic flow in a channel and the equivalent barotropic flow on the sphere. The vertical jet profile is more unstable the lower the jet maximum, this means that the (linear) wind-shear on the bottom side of the jet, where the static stability is smallest, dominates the stability properties of the jet. In case of a barotropic jet on the sphere we find the flow to be more unstable the larger the shear. The flow is more stable the more pole-ward the jet, which indicates that the Coriolis force tends to stabilize the flow.

In all 3 cases, it was found that the most unstable modes have zonal wavenumbers 5–10, corresponding to wavelengths of 2000–4000 km. This is in agreement with the findings from the simpler models by Eady, Charney, Kuo and others. The baroclinic jet is more unstable than the barotropic for conditions realistic to the atmosphere.

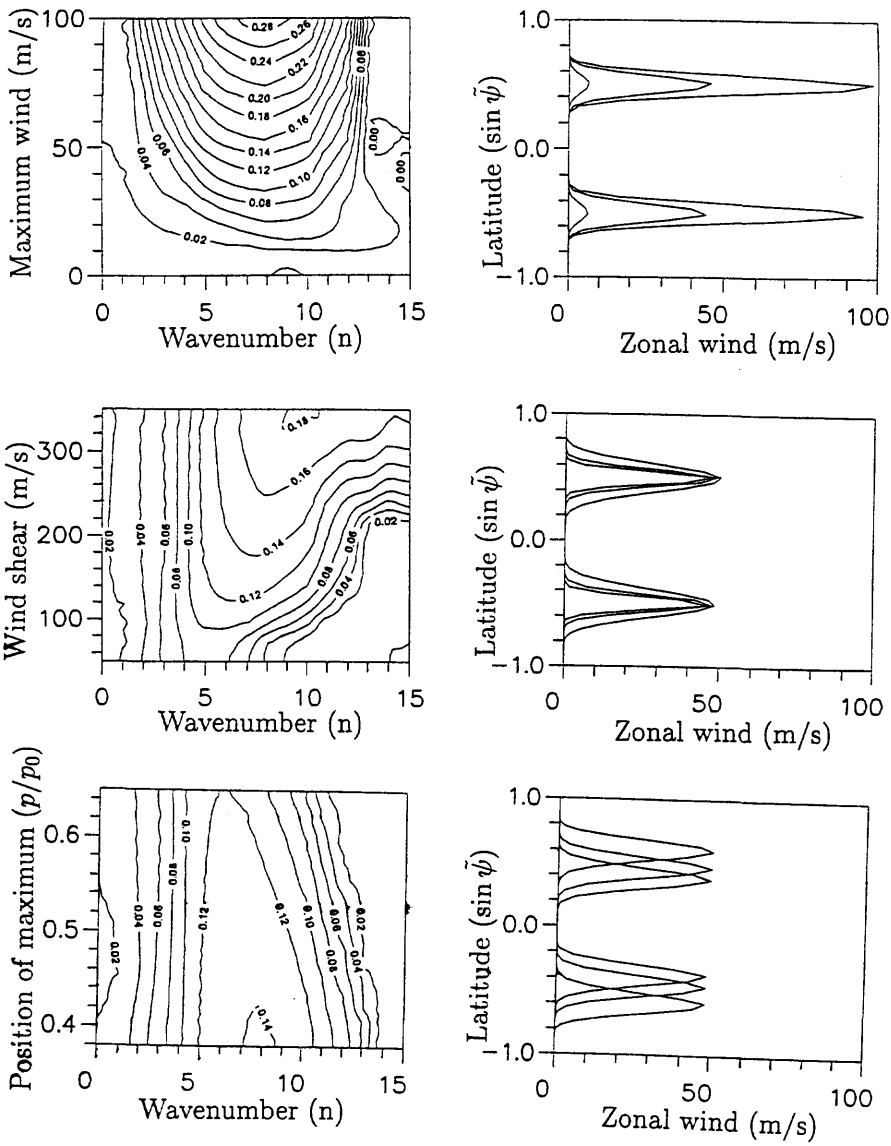

Fig. 6. Barotropic instability: same as Fig. 5 for the flow on the sphere. The perturbation vertical wavenumber is 0, corresponding to the external mode.

It is remarkable that the results from such simple 1-dimensional models investigated here are in very good agrement with the general picture obtained from much more complicated 3-dimensional analyses. The simplicity of this study enables us to clearly investigate the isolated effect of baroclinic or barotropic instabilities of typical jets.

6. Acknowledgements

Thanks to Professor Aksel Wiin-Nielsen for urging me to do this work; thanks also to Lone Gross for bibliographic assistance. The work was funded by the Carlsberg Foundation.

REFERENCES

Burger, A. P. 1962. On the non-existence of critical wavelengths in a continuous baroclinic stability problem. *J. Atmos. Sci.* **19**, 31–38.

Charney, J. G. 1947. The dynamics of long waves in baroclinic westerly currents. *Jour. Meteor.* **4**, 135–162.

Eady, E. T. 1949. Long waves and cyclonic waves. *Tellus* **1**, 33–52.

Frederiksen, J. S. 1978. Instability of planetary waves and zonal flows in two-layer models on a sphere. *Q. J. Roy. Meteor. Soc.* **104**, 841–872.

Green, J. A. S. 1960. A problem in baroclinic stability. *Q. J. Roy. Meteor. Soc.* **86**, 237–251.

Grotjahn, R. 1984. Baroclinic instability in a long wave environment. Part I: Review. *Quart. J. Roy. Meteor. Soc.* **110**, 663–668.

Grotjahn, R. 1987. Three-dimensinal linear instability on a sphere: resolution experiments with a model using vertical orthorgonal basis functions. *J. Atmos. Sci.* **44**, 3734–3752.

Kasahara, A. and Tanaka, H. L. 1989. Application of vertical normal mode expansion to problems of baroclinic instability. *J. Atmos. Sci.* **46**, 489–510.

Kuo, H. L. 1973. Dynamics of quasigeostrophic flows and instability theory. *Advances in Applied Mechanics* **13**, 248–330.

Kuo, H. L. 1979. Baroclinic instabilities of linear and jet profiles in the atmosphere. *J. Atmos. Sci.* **36**, 2360–2378.

Palmer, T. N., Buizza, R., Molteni, F., Chen, Y-Q. and Corti, S. 1994. Singular vectors and the predictability of weather and climate. *Phil. Trans. R. Soc. Lond. A* **348**, 459–475.

Pedlosky, J. 1987. *Geophysical fluid dynamics.* Springer-Verlag, 710 pp.

Simmons, A. J. and Hoskins, B. J. 1976. Baroclinic instability on the sphere: normal modes of the primitive and quasi-geostrophic equations. *J. Atmos. Sci.* **33**, 1454–1477.

Toth, Z. and Kalney, E. 1993. Ensamble forecasting at NMC: the generation of perturbations. *Bull. Amer. Meteor. Soc.* **74**, 2317–2330.

Wiin-Nielsen, A. and Marshall, H, 1990. On the structure of transient atmospheric waves. Part III. *Atmósfera* **3**, 73–109.